Lithium alloy negative electrodes formed from convertible oxides

Robert A. Huggins

Technical Faculty, Christian-Albrechts-University, D-24143 Kiel, Germany

Abstract

Fuji Photo Film Co. recently announced the development of lithium batteries employing oxide negative electrodes. Under near-equilibrium conditions these oxides are converted to lithium alloys during the first charging cycle. Thereafter, the properties should be essentially those of the resulting binary lithium alloys. The basic principles involved in the use of alloys as negative electrodes, as well as the conversion of oxides to alloys, are presented. Available data on the behavior of a number of lithium alloys and binary oxides as negative electrodes in lithium systems are also included. The lithium–tin system is discussed in some detail as it is a particularly relevant example. © 1998 Published by Elsevier Science B.V. All rights reserved.

Keywords: Tin oxide; Alloy anode; Composite

1. Introduction

The recent announcement by Fuji Photo Film Co. of the development of a new generation of lithium batteries based upon the use of an amorphous tin-based composite oxide in the negative electrode [1–3], and the establishment of a new company, Fujifilm Celltec Co., to produce products based upon this approach, has caused a renewed interest in non-carbonaceous lithium alloy electrodes.

It is claimed that these electrodes have a volumetric capacity of 3200 A h/l, which is four times that commonly achieved with carbon-based negative electrodes, and a specific capacity of 800 mA h/g, twice that generally found in carbon-containing negative electrodes.

This paper will discuss the basic principles involved in the use of both alloys and convertible oxides as negative electrodes, as well as presenting some of the available data on such systems. Since the lithium–tin system is of special current interest, it will be given special attention.

2. Use of lithium alloys as negative electrodes in lithium-based systems

Attention has been given to the use of lithium alloys as an alternative to elemental lithium for some time. Groups working on batteries with molten salt electrolytes that operate at temperatures of 400–450°C, well above the melting point of lithium have been especially interested in this possibility. Two major directions evolved. One involved the use of lithium– aluminum alloys [4,5], whereas another was concerned with lithium–silicon alloys [6–8].

Whereas this approach can avoid the problems related to lithium melting, there are always at least two disadvantages related to the use of alloys. Because they reduce the activity of the lithium they

necessarily reduce the cell voltage. In addition, the presence of additional species that are not directly involved in the electrochemical reaction always results in additional weight, and generally, volume. Thus, the maximum theoretical values of the specific energy and the energy density are always reduced compared to what might be attained with pure lithium.

Another potential disadvantage is that there is often a substantial change in specific volume upon charging and discharging alloy electrode reactants. This can lead to loss of electrical contact, and thus capacity loss, as well as macroscopic dimensional problems within the cell structure.

The first use of lithium alloys as negative electrodes in commercial batteries to operate at ambient temperatures was the employment of Wood's metal alloys in lithium-conducting button type cells by Matsushita in Japan. Development work on the use of these alloys started in 1983 [9], and they became commercially available somewhat later.

It was also shown in 1983 [10] that lithium can be reversibly inserted into graphite at room temperatures when using a polymeric electrolyte. Prior experiments with liquid electrolytes were unsuccessful due to co-intercalation of species from the organic electrolytes that were used at that time. This problem has been subsequently solved by the use of other electrolytes, and a large amount of attention has been given to the development of graphites and related carbon-containing materials for use as negative electrode materials in lithium batteries in recent years. This is due in large part to the successful development by SONY of commercial rechargeable batteries containing negative electrodes based upon materials of this family.

Since this topic is treated in detail elsewhere, only a few points will be briefly discussed here. One is that the behavior of these materials is very dependent upon the details of both the nanostructure and the microstructure. Therefore, the composition as well as thermal and mechanical treatment play especially important roles in determining the resulting thermodynamic and kinetic properties. Materials with a more graphitic structure have more negative potentials, whereas those with less well organized structures typically operate over much wider potential ranges, resulting in a cell voltage that is both lower and more state-of-charge dependent.

Another important consideration in the use of carbonaceous materials as negative electrodes in lithium cells is the common observation of a considerable loss of capacity during the first charge–discharge cycle due to irreversible lithium absorption into the structure. This has the distinct disadvantage that it requires that an additional amount of lithium be initially present in the cell. If this irreversible lithium is supplied by the positive electrode, this means that an extra amount of the positive electrode reactant material must be put into the cell during its fabrication. As the positive electrode reactant materials often have relatively low specific capacities, e.g. around 140 mA h/g, this irreversible capacity in the negative electrode leads to a requirement for an appreciable amount of extra material weight and volume in the total cell.

This matter of first-cycle capacity loss is also of concern in the case of the use of convertible oxides, as will be shown later.

There are some other matters that should be considered when comparing metallic lithium alloys with the lithium–carbons. The specific volume of some of the metallic alloys can be considerably lower than that of the carbonaceous materials. As will be seen later, it is also possible by selection among the metallic materials to find good kinetics and electrode potentials that are sufficiently far from that of pure lithium that there is a much lower possibility of the potentially dangerous formation of dendrites or filamentary deposits of pure lithium under rapid recharge conditions.

3. Alloys formed in-situ from convertible oxides

If an electrode initially contains an oxide that is less stable than lithium oxide, there will be a thermodynamic driving force for a displacement reaction in which Li_2O will be formed at the expense of the prior oxide. We can take an electrode initially containing SnO as an example. If we introduce lithium into it there will be a displacement reaction in which Li_2O will be formed at the expense of the SnO.

$$2Li + SnO = Li_2O + Sn$$
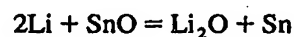
The difference in the values of their Gibbs free

energies of formation (-562.1 kJ/mol for Li_2O and -256.8 kJ/mol in the case of SnO) provides the driving force. In this case it is quite strong, equivalent to 1.58 V.

The other product will be elemental Sn, and as additional Li is brought into the electrode this Sn will tend to react further to form the various Li–Sn alloys that exist in the lithium–tin phase diagram. This simplified picture is consistent with what has already been found in experiments of this general type [11,12].

If the formation of Li_2O is not reversible, the electrode will maintain a composite microstructure and behave as a binary lithium–tin alloy after the first cycle. This initial Li_2O formation represents a significant initial capacity loss. Significant first cycle capacity losses are also generally found in lithium–carbon electrodes, although the mechanism is different.

4. Thermodynamic basis for electrode potentials and capacities under conditions in which complete equilibrium can be assumed

The general thermodynamic treatment of binary systems which involve the incorporation of an electroactive species into a solid alloy electrode under the assumption of complete equilibrium was presented by Weppner and Huggins [13–15]. Under these conditions the Gibbs Phase Rule specifies that the electrochemical potential varies with composition in the single phase regions of a binary phase diagram, and is composition-independent in two-phase regions if the temperature and total pressure are kept constant.

Thus, the variation of the electrode potential during discharge and charge, as well as the phases present and the charge capacity of the electrode, directly reflect the thermodynamic properties of the alloy system.

A series of experiments have been undertaken to evaluate the relevant thermodynamic properties of a number of binary lithium alloy systems. The early work was directed toward determination of their behavior at about 400°C because of interest in their potential use as components in molten salt batteries operating in that general temperature range. Data for a number of binary lithium alloy systems at about

400°C are presented in Table 1. These were mostly obtained by the use of an experimental arrangement employing the LiCl–KCl eutectic molten salt as a lithium-conducting electrolyte.

It was shown some time ago that one can also use a similar thermodynamic approach to explain and/or predict the composition-dependence of the potential of electrodes in ternary systems [16–19]. This followed from the development of the analysis methodology for the determination of the stability windows of electrolyte phases in ternary systems [20]. In these cases, one uses isothermal sections of ternary phase diagrams, the so-called Gibbs triangles, upon which to plot compositions. In ternary systems, the Gibbs Phase Rule tells us that three-phase equilibria will have composition-independent intensive properties, i.e. activities and potentials. Thus, compositional ranges that span three-phase regions will lead

Table 1

Plateau potentials and composition ranges of a number of binary lithium alloys at elevated temperatures

Voltage vs Li	System	Range of y	Temp. (°C)	Reference
0.047	Li_ySi	3.25–4.4	400	[29]
0.058	Li_yCd	1.65–2.33	400	[21]
0.080	Li_yIn	2.08–2.67	400	[41]
0.089	Li_yPb	3.8–4.4	400	[42]
0.091	Li_yGa	1.53–1.93	400	[43]
0.122	Li_yGa	1.28–1.48	400	[43]
0.145	Li_yIn	1.74–1.92	400	[41]
0.156	Li_ySi	2.67–3.25	400	[29]
0.170	Li_ySn	3.5–4.4	400	[30]
0.237	Li_yPb	3.0–3.5	400	[42]
0.271	Li_yPb	2.67–3.0	400	[42]
0.283	Li_ySi	2–2.67	400	[29]
0.283	Li_ySn	2.6–3.5	400	[30]
0.300	Li_yAl	0.08–0.9	400	[27]
0.332	Li_ySi	0–2	400	[29]
0.373	Li_yCd	0.33–0.45	400	[21]
0.375	Li_yPb	1.1–2.67	400	[42]
0.387	Li_ySn	2.5–2.6	400	[30]
0.430	Li_ySn	2.33–2.5	400	[30]
0.455	Li_ySn	1.0–2.33	400	[30]
0.495	Li_yIn	1.2–0.86	400	[41]
0.507	Li_yPb	0–1.0	400	[42]
0.558	Li_yCd	0.12–0.21	400	[21]
0.565	Li_yGa	0.15–0.82	400	[43]
0.570	Li_ySn	0.57–1.0	400	[30]
0.750	Li_yBi	1.0–2.82	400	[15]
0.875	Li_ySb	2.0–3.0	400	[15]
0.910	Li_ySb	0–2.0	400	[15]

to potential plateaus at constant temperature and pressure.

This thermodynamically-based methodology provides predictions of the lithium capacities in addition to the electrode potentials of the various three-phase equilibria under conditions of complete equilibrium.

From a practical standpoint, the most useful materials for use as negative electrodes in lithium systems would be those with quite negative potentials, so as to give high cell voltages, that also have large capacities for lithium. However, it must be recognized that the materials with the most negative potentials, and thus the highest lithium activities, will be the most reactive, and thus will be more difficult to handle than those whose potentials are somewhat farther from that of pure lithium. There is also the potential danger of the formation of elemental lithium during rapid recharge of such materials.

5. Structural aspects and the possibility of selective equilibrium

If we look at the mechanistic and crystallographic aspects of the operation of polycomponent electrodes, we see that the incorporation of electroactive species such as lithium into a crystalline electrode can occur in two basic ways. In the examples discussed above, and in which complete equilibrium is assumed, the introduction of the guest species can either involve a simple change in the composition of an existing phase by solid solution, or it can result in the formation of new phases with different crystal structures from that of the initial host material. When the identity and/or amounts of phases present in the electrode change, the process is described as a reconstitution reaction. That is, the microstructure is reconstituted.

In the simple case of a reconstitution reaction in which the incorporation of additional electroactive species occurs by the nucleation and growth of a new phase the relative amount of this new phase with a higher solute content increases. If the initial phase and the new phase are in local equilibrium, the respective compositions at their joint interface do not change with the extent of the reaction. The amounts of the phases, determined by the motion of the interfaces between these phases, are related to the

lengths of the two-phase constant potential plateaus in binary systems, and of the three-phase constant potential plateaus in ternary systems, and these are, in turn, determined by the extent of the corresponding regions in the relevant phase diagrams.

In many systems, both single phase and polyphase behavior are found in different composition ranges. Intermediate, as well as terminal, phases often have been found to have quite wide ranges of composition. Examples are the broad Zintl phases found in several of the binary lithium systems studied by Wen [21].

The second way in which an electroactive species such as lithium can be incorporated into the structure of an electrode is by a topotactic insertion reaction. In this case the guest species is relatively mobile and enters the crystal structure of the host phase such that no significant change in the structural configuration of the host lattice occurs.

Thus, the result is the formation of a single phase solid solution. The insertion of additional guest species involves only a change in the overall (and thus also the local) composition of the solid solution, rather than the formation of additional phases.

From a thermodynamic viewpoint, there is selective equilibrium, rather than complete equilibrium, under conditions in which this type of reaction occurs. We can assume equilibrium in the sublattice of the mobile solute species, but not in the host substructure, as strong bonding makes atomic rearrangements relatively sluggish in that part of the crystal structure.

In general, equilibrium within the guest species sublattice results in their being randomly arranged among the various interstititial locations within the host structure. There are, however, a number of cases in which the guest species are distributed among their possible sites within the host structure in an ordered, rather than random, manner. There can be different sets of these ordered sites, each having the thermodynamic characteristics of a separate phase. Thus, as the concentration of guest species is changed, such materials can appear thermodynamically to go through a series of phase changes, even though the host structure is relatively stable. An example of this type of behavior was demonstrated in the case of lithium insertion into a potassium tungsten oxide [22].

The thermodynamic properties of topotactic inser-

tion reaction materials with selective equilibrium are quite different from those of materials in which complete equilibrium can be assumed, and reconstitution reactions take place. Instead of flat plateaus related to polyphase equilibria, the composition-dependence of the potential generally has a flat S-type form.

Under near-equilibrium conditions the shape of this curve is related to two contributions, the compositional-dependence of the configurational entropy of the guest ions, and the contribution to the chemical potential from the electron gas [23].

The configurational entropy of the mobile guest ions, assuming random mixing, and a concentration x, residing in x° lattice sites of equal energy, is

$$S = - R \ln[x/(x^\circ - x)]$$

There is also a small contribution from thermal entropy, but this can be neglected.

If we can assume that the electrode material is a good metal, and the electronic gas is fully degenerate, the chemical potential of the electrons is given by the Fermi level, E_μ, which can be written as

$$E_F = (\text{Constant})((x)^{2/3}/m^*)$$

where m^* is the effective mass of the electrons.

Thus, instead of having a series of plateaus, the variation of the electrode potential with composition of single phase random insertion reaction electrodes should be of the form

$$E = A + Bx^{2/3} - (RT/nF) \ln(x/(1 - x))$$

where A and B are constants.

6. Kinetic aspects

In addition to the questions of the potentials and capacities of electrodes, which are essentially thermodynamic considerations, practical utilization of alloys as electrodes also requires attractive kinetic properties.

The primary question is the rate at which the mobile guest species can be added to, or deleted from, the host microstructure. In many situations the critical problem is the transport within a particular phase under the influence of gradients in chemical composition, rather than kinetic phenomena at the

electrolyte/electrode interface. In this case, the governing parameter is the chemical diffusion coefficient of the mobile species, which relates to its transport in a chemical concentration gradient.

Experimental measurement of diffusion in metals has often involved the use of radioactive tracers. However, the quantity that is measured by this method is related to the self-diffusion coefficient, a measure of interdiffusion in the absence of a concentration gradient. In intermediate phases in alloy systems this can be significantly different from the chemical diffusion coefficient. In one example, this difference was shown to be a factor of 70 000 [24].

It is thus much better to measure the chemical diffusion coefficient directly. Descriptions of electrochemical methods for doing this, as well as the relevant theoretical background, can be found in the literature [25,26].

7. Examples of lithium alloy systems at elevated temperatures

Because of the interest in its use in elevated temperature molten salt electrolyte batteries, one of the first binary alloy systems studied in detail was the lithium–aluminum system. The potential-composition behavior shows a long plateau between the lithium-saturated terminal solid solution and the intermediate beta phase 'LiAl', and a shorter one between the composition limits of the beta and gamma phases, as well as composition-dependent values in the single phase regions [27]. This is as expected for a binary system with complete equilibrium. The potential of the first plateau varies linearly with temperature [27].

Because chemical diffusion in the beta phase determines the kinetic behavior of these electrodes when lithium is added, this was investigated in detail using four different electrochemical techniques [26,27]. It was found that chemical diffusion is remarkably fast in this phase, and that the activation energy attains very low values on the lithium-poor side of the composition range. In addition to this work on the beta phase, both the thermodynamic and kinetic properties of the terminal solid solution region, which extends to about nine atomic percent lithium at 423°C, were also investigated in detail [28].

The lithium–silicon system has also been of interest for use in the negative electrodes of elevated temperature molten salt electrolyte lithium batteries. A composition containing 44 wt. % Li, where Li/ Si = 3.18, has been used in commercial thermal batteries developed for military purposes. Experiments have been performed to study both the thermodynamic and kinetic properties of compositions in this system [29]. The commercial electrode composition sits upon a two-phase plateau at a potential 158 mV positive of pure lithium. As lithium is removed the overall composition will first follow that plateau. The potential will then become more positive as it traverses the other plateaus at 288 and 332 mV versus lithium in order. As a result, the cell voltage will decrease during the discharge, regardless of the behavior of the positive electrode.

The lithium–tin binary system is somewhat more complicated, as there are six intermediate phases. A thorough study of the thermodynamic properties of this system was undertaken [30]. This included measurements of the potential-composition behavior, as well as the chemical diffusion coefficient, and its composition dependence, in each of the intermediate phases at 415°C [31]. It was found that chemical diffusion is reasonably fast in all of the intermediate phases in this system. The self diffusion coefficients are all high and of the same order of magnitude. However, due to its large value of thermodynamic enhancement factor W, the chemical diffusion coefficient in the phase $Li_{13}Sn_5$ is extremely high, approaching 10^{-3} cm^2/s, which is about two orders of magnitude higher than that in typical liquids.

8. Lithium alloys at lower temperatures

A smaller number of binary lithium systems have also been investigated at lower temperatures. This has involved measurements using $LiNO_3$–KNO_3 molten salts at about 150°C [32], as well as experiments with organic solvent-based electrolytes at ambient temperatures [33,34].

The lithium–tin system has been investigated at room temperature. There are five constant-potential plateaus. It was found that the kinetics on the longest plateau, from $x = 0.8$ to 2 in Li_xSn, are quite favorable, even at quite high currents [33]. The com-

Table 2
Plateau potentials and composition ranges of some lithium alloys at low temperatures

Voltage vs Li	System	Range of y	Temp. (°C)	Reference
0.005	Li_yZn	1–1.5	25	[34]
0.055	Li_yCd	1.5–2.9	25	[34]
0.157	Li_yZn	0.67–1	25	[34]
0.219	Li_yZn	0.5–0.67	25	[34]
0.256	Li_yZn	0.4–0.5	25	[34]
0.292	Li_yPb	3.2–4.5	25	[34]
0.352	Li_yCd	0.3–0.6	25	[34]
0.374	Li_yPb	3.0–3.2	25	[34]
0.380	Li_ySn	3.5–4.4	25	[33]
0.420	Li_ySn	2.6–3.5	25	[33]
0.449	Li_yPb	1–3.0	25	[34]
0.485	Li_ySn	2.33–2.63	25	[33]
0.530	Li_ySn	0.7–2.33	25	[33]
0.601	Li_yPb	0–1	25	[34]
0.660	Li_ySn	0.4–0.7	25	[33]
0.680	Li_yCd	0–0.3	25	[34]
0.810	Li_yBi	1–3	25	[33]
0.828	Li_yBi	0–1	25	[33]
0.948	Li_ySb	2–3	25	[33]
0.956	Li_ySb	1–2	25	[33]

position-dependence of the potential of the most lithium-rich phase, $Li_{4.4}Sn$ ($Li_{22}Sn_5$), was determined. The chemical diffusion coefficient in that phase has also been evaluated and found to be quite high [35]. The chemical diffusion coefficient was also measured in two other Li–Sn phases.

Comparable information on the Li–Bi, Li–Sb, Li–Zn, Li–Cd and Li–Pb alloy systems has also been obtained at room temperature [33–35]. Plateau potentials and composition ranges of some lithium alloys at ambient temperature are presented in Table 2.

9. Composite structure electrodes

9.1. Mixed-conductor matrix electrode structures

In order to be able to achieve appreciable macroscopic current densities while maintaining low local microscopic charge and particle flux densities, many battery electrodes that are used in conjunction with liquid electrolytes are produced with porous microstructures containing very fine particles of the solid

reactant materials. This high reactant surface area porous structure is permeated with the electrolyte.

This porous fine-particle approach has several characteristic disadvantages. Among these are difficulties in producing uniform and reproducible microstructures, and limited mechanical strength when the structure is highly porous. In addition, they often suffer Ostwald ripening, sintering, or other time-dependent changes in both microstructure and properties during cyclic operation.

A quite different approach [36–38] involves the use of a dense solid electrode with a composite microstructure in which particles of the reactant phase are finely dispersed within a solid electronically-conducting matrix in which the electroactive species is also mobile. There is thus a large internal reactant/mixed-conducting matrix interfacial area. The electroactive species is transported through the solid matrix to this interfacial region, where it undergoes the chemical part of the electrode reaction. Since the matrix material is also an electronic conductor, it can also act as the electrode's current collector. The electrochemical part of the reaction takes place on the outer surface of the composite electrode.

When such an electrode is discharged by deletion of the electroactive species, the residual particles of the reactant phase remain as relics in the microstructure. This provides fixed permanent locations for the reaction to take place during following cycles, when the electroactive species again enters the structure. Thus, this type of configuration can provide a mechanism for the achievement of true microstructural reversibility.

In order for this concept to be applicable, the matrix and the reactant phase must be thermodynamically stable in contact with each other. One can evaluate this possibility if one has information about the relevant phase diagram – which typically involves a ternary system – as well as the titration curves of the component binary systems. In a ternary system, the two materials must lie at corners of the same constant-potential tie triangle in the relevant isothermal ternary phase diagram in order to not interact. The potential of the tie triangle determines the electrode reaction potential, of course.

An additional requirement is that the reactant material have two phases present in the tie triangle,

but the matrix phase only one. This is another way of saying that the stability window of the matrix phase must span the reaction potential, but that the binary titration curve of the reactant material must have a plateau at the tie triangle potential. It has been shown that one can evaluate the possibility that these conditions are met from knowledge of the binary titration curves, without having to do a large number of ternary experiments.

The kinetic requirements for a successful application of this concept are readily understandable. The primary issue is the rate at which the electroactive species can reach the matrix/reactant interfaces. The critical parameter is the chemical diffusion coefficient of the electroactive species in the matrix phase. This can be determined by various techniques, as discussed above.

The first example that was demonstrated was the use of the phase with the nominal composition $Li_{2.6}Sn$ ($Li_{13}Sn_5$) as the matrix, in conjunction with reactant phases in the lithium–silicon system at temperatures near 400°C. This is an especially favorable case, due to the high chemical diffusion coefficient of lithium in the $Li_{2.6}Sn$ phase.

The phase $Li_{2.6}Sn$ is stable over a potential range that includes the upper two-phase reconstitution reaction plateau in the lithium–silicon system. Therefore, lithium can react with Si to form the phase $Li_{1.71}Si$ ($Li_{12}Si_7$) inside an all-solid composite electrode containing the $Li_{2.6}Sn$ phase, which acts as a lithium-transporting, but electrochemically inert matrix. Relatively small polarization has been observed during the charge and discharge of this electrode, even at relatively high current densities. There is a small, but obvious, potential overshoot due to the free energy involved in the nucleation of a new second phase if the reaction goes to completion in each direction. On the other hand, when the composition was not driven quite so far, this nucleation-related potential overshoot did not appear.

This concept has also been demonstrated at ambient temperature in the case of the Li–Sn–Cd system [39,40]. The phase stability diagram for this ternary system was calculated. The composition-dependences of the potentials in the two binary systems are such that the phase $Li_{4.4}Sn$, which has fast chemical diffusion for lithium at ambient temperatures, is stable at the potentials of two of the

Li–Cd reconstitution reaction plateaus. It can therefore can be used as a matrix phase. The behavior of this composite electrode, in which Li reacts with the Cd phases inside of the Li–Sn phase, was demonstrated experimentally.

In order to achieve good reversibility, the composite electrode microstructure must have the ability to accommodate any volume changes that might result from the reaction that takes place internally. This can be taken care of by clever microstructural design and alloy fabrication techniques.

9.2. Solid electrolyte matrix electrode structures

In solid state systems it is often advantageous to have some of the electrolyte material mixed in with the reactant, and this has been done to enhance the kinetic behavior in a number of cases. There are two general advantages that result from doing this. One is that the contact area between the electrolyte phase and the electrode phase, the electrochemical interface, is greatly increased. The other is that the presence of the electrolyte material changes the thermal expansion characteristics of the electrode structure so as to be closer to that of the pure electrolyte. By doing so, the stresses that arise as the result of a difference in the expansion coefficients of the two adjacent phases that can cause mechanical separation of the interface are reduced.

10. The lithium–tin oxide system

The recently announced Fuji Photo Film development is said to involve the use of an amorphous tin-based composite oxide. We can assume that this is an example of a convertible oxide electrode, and that reaction with lithium on the first charge cycle results in the formation of a microstructure containing fine dispersions of both Li–Sn alloys and Li_2O. The latter is known to be a lithium-transporting solid electrolyte. Thus, these electrodes can be thought of as having a composite microstructure with an electrolyte as well as the reactant phase.

We can look briefly at two simple cases to see the effect of starting with a convertible oxide. Let us consider the use of either SnO_2 or SnO as precursors for the in-situ formation of Li–Sn alloys.

If the simplifying assumption is made that there are no stable ternary phases, a simple isothermal phase stability diagram can be constructed to use as a thinking tool in working out the properties of this system. A simplified version of such a diagram is shown in Fig. 1.

If lithium reacts with one of the tin oxide phases, the overall composition will move toward the Li corner of the ternary diagram, and under conditions close to equilibrium, it will move along one of the dotted lines shown in that figure.

Gibbs free energy of formation data allow us to determine the phases that are stable with each other and the reactions that will tend to take place when lithium is introduced into an electrode. The results are shown in that figure, and we see that the overall composition will move through a series of three-phase triangles, crossing two-phase tie lines between them.

When three phases are present in a ternary system and the temperature and the overall pressure are held constant, there are no degrees of freedom, according to the Gibbs Phase Rule. This means that the electrical potential must be independent of composition, i.e. there will be a potential plateau. This potential can be calculated from the Gibbs free energy change involved in the virtual reaction that takes place within the three-phase region.
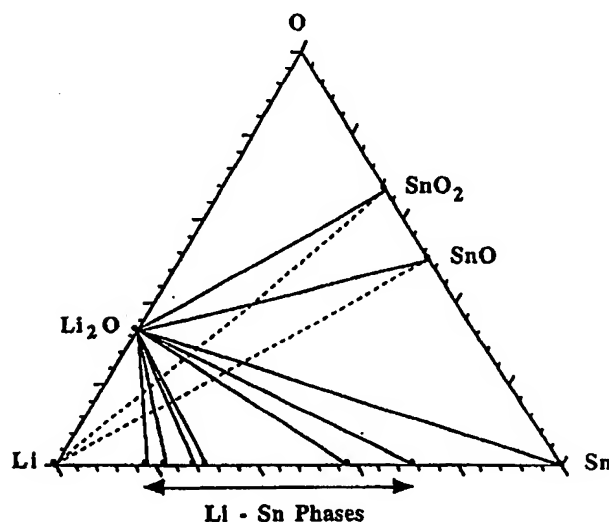

Fig. 1. Simplified isothermal phase stability diagram for the Li–Sn–O system, assuming that there are no stable ternary phases.
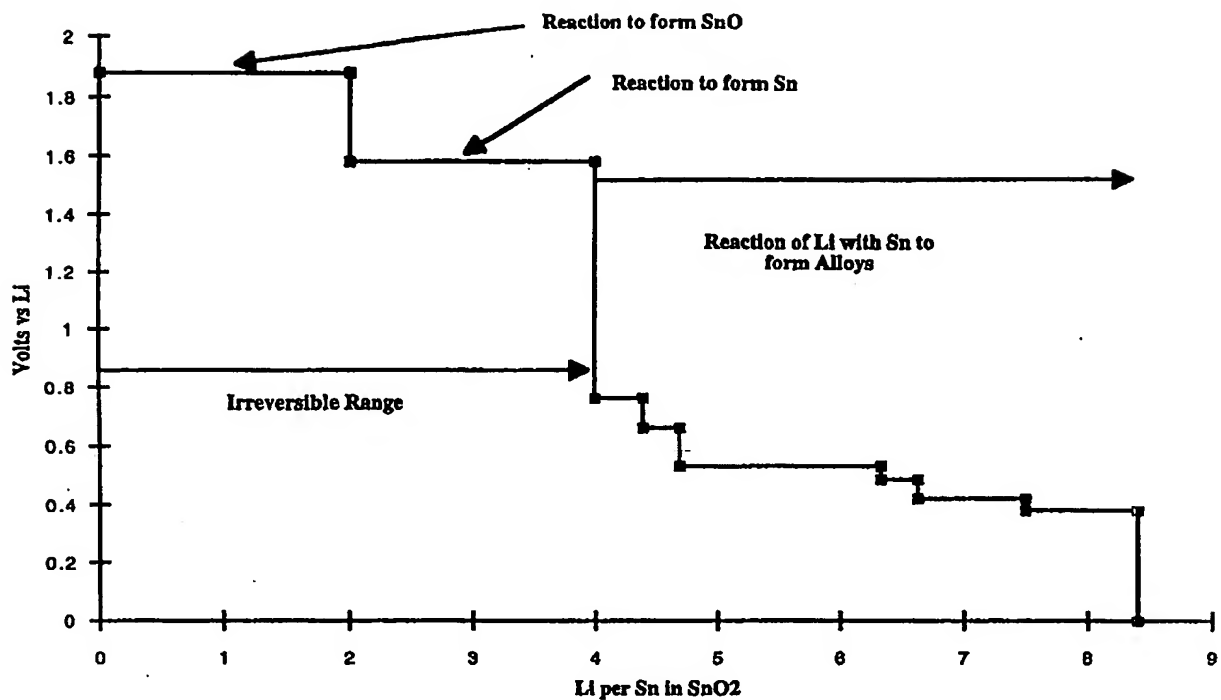
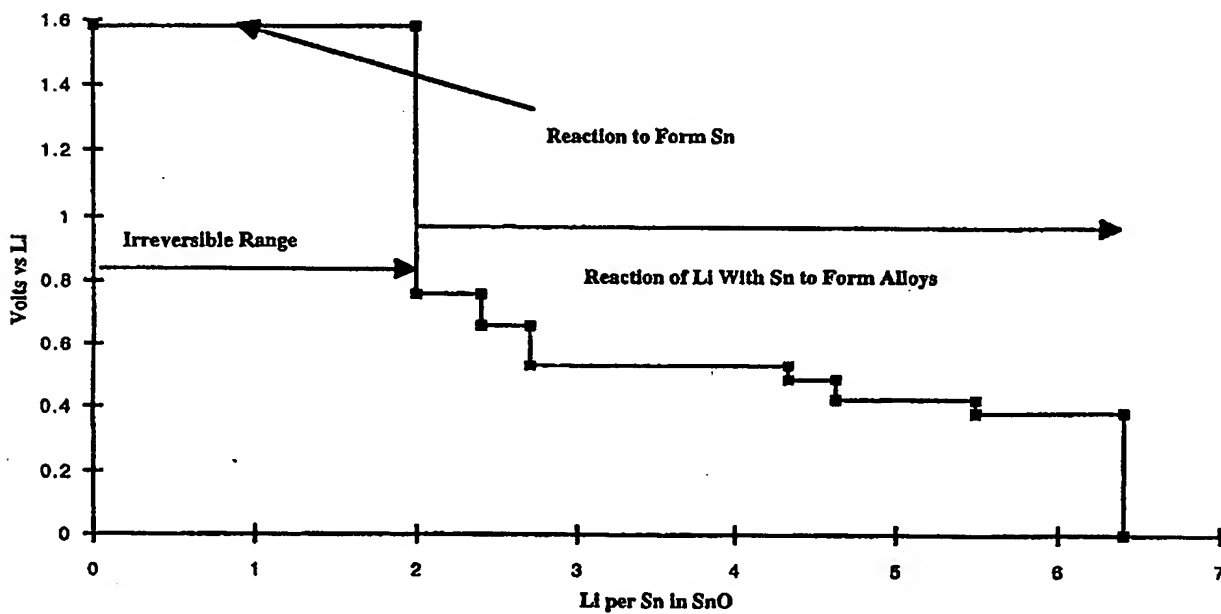Fig. 2. Theoretical titration curve for reaction of lithium with SnO_2.

Fig. 3. Theoretical titration curve for reaction of lithium with SnO.

Table 3

Equilibrium potentials of plateaus in three-phase regions in the Li–Sn–O ternary system at ambient temperature

Three-phase equilibrium	Potential (V vs Li)
$Li_2O-O_2-SnO_2$	2.912
Li_2O-SnO_2-SnO	1.880
$Li_2O-SnO-Sn$	1.582
$Li_2O-Sn-Li_{0.4}Sn$	0.760
$Li_2O-Li_{0.4}Sn-Li_{0.714}Sn$	0.660
$Li_2O-Li_{0.714}Sn-Li_{2.33}Sn$	0.530
$Li_2O-Li_{2.33}Sn-Li_{2.6}Sn$	0.485
$Li_2O-Li_{2.6}Sn-Li_{3.5}Sn$	0.420
$Li_2O-Li_{3.5}Sn-Li_{4.4}Sn$	0.380

We can express this result in terms of a theoretical electrochemical titration curve, in which the potential (V vs Li) is plotted versus the composition. The result is a series of constant-voltage plateaus as the composition moves across the three-phase regions of the diagram. These are shown for two cases, starting with SnO_2 and starting with SnO in Figs. 2 and 3.

Experimental values of the potentials of the lithium–tin plateaus at room temperature [33], along with calculated values based upon the thermodynamic data for the oxides, are included in Table 3.

11. Irreversible and reversible capacities

We see that if we start with SnO_2, two lithiums will initially react to form Li_2O and SnO at a potential of 1.88 V vs Li. Following this, an additional two lithiums will react with the SnO to form more Li_2O and Sn at a potential of 1.582 V vs Li. If we can assume that these two reactions are irreversible, and that we cannot remove this lithium to decompose the Li_2O and reform the tin oxides, four lithium atoms are consumed if the initial oxide is SnO_2. Two lithium atoms react irreversibly if the initial oxide is SnO. This represents a large irreversible capacity, 711.3 mA h/g of SnO_2 if the electrode starts as SnO_2, and 397.9 mA h/g of SnO if the electrode is initially SnO.

This irreversible lithium must come from somewhere in the cell, i.e. from the positive electrode. Thus, a significant amount of extra lithium-containing positive electrode reactant must be present when the cell is fabricated.

Now let us consider the active reversible capacity, rather than the irreversible capacity. This is the capacity that is obtained by the reaction of additional lithium with the tin that resulted from the earlier irreversible reactions.

We see from the theoretical titration diagrams that an additional 4.4 lithiums can react in each case, assuming that the overall composition starts with pure tin after the conversion of the oxides. If we assume that this is all reversible, and that the electrode starts as SnO_2, this is a reversible capacity of 782 mA h/g of SnO_2. On the other hand, if it starts as SnO, the reversible capacity is 875 mA h/g of SnO.

Similar irreversible and reversible capacities are theoretically found in other convertible oxide systems. Data on a few examples are shown in Table 4.

Table 4

Theoretical irreversible and reversible capacities of several convertible oxides

Starting oxide	Reversible capacity mA h/g oxide	Irreversible capacity mA h/g oxide	Total capacity mA h/g oxide	Ratio rev/total
SnO	875.36	398	1273	0.69
SnO_2	782.43	711	1494	0.52
ZnO	493.92	659	1152	0.43
CdO	605.25	417	1023	0.59
PbO	540.32	240	780	0.69

References

[1] Fujifilm, Internet: http://www.fujifilm.co.jp/eng/news_e/nr079.html, (1996).

[2] Y. Idota, N. Nishima, Y. Miyaki, T. Kubota, T. Miyasaki, Canadian Patent Appl. 2,134,053 (1994).

[3] Y. Idota, A. Matsufuji, Y. Maekawa, T. Miyasaki, Science 276 (1997) 1395.

[4] N.P. Yao, L.A. Heredy, R.C. Saunders, J. Electrochem. Soc. 118 (1971) 1039.

[5] E.C. Gay, et al., J. Electrochem. Soc. 123 (1976) 1591.

[6] S.C. Lai, J. Electrochem. Soc. 123 (1976) 1196.

[7] R.A. Sharma, R.N. Seefurth, J. Electrochem. Soc. 123 (1976) 1763.

[8] R.N. Seefurth, R.A. Sharma, J. Electrochem. Soc. 124 (1977) 1207.

[9] H. Ogawa, in: Proceedings of 2nd International Meeting on Lithium Batteries, Elsevier Sequoia, 1984, p. 259.

[10] R. Yazami, P. Touzain, J. Power Sources 9 (1983) 365.

[11] I.A. Courtney, J.R. Dahn, J. Electrochem. Soc. 144 (1997) 2045.

[12] I.A. Courtney, J.R. Dahn, J. Electrochem. Soc. 144 (1997) 2943.

[13] W. Weppner, R. A. Huggins, in: J.D.E. McIntyre, S. Srinivasan, F.G. Will (Eds.), Proceedings of the Symposium on Electrode Materials and Processes for Energy Conversion and Storage, Electrochemical Society, 1977, p. 833.

[14] W. Weppner, R.A. Huggins, Z. Phys. Chem. N.F. 108 (1977) 105.

[15] W. Weppner, R.A. Huggins, J. Electrochem. Soc. 125 (1978) 7.

[16] C.M. Luedecke, J.P. Doench, R.A. Huggins, in: Z.A. Munir, D. Cubicciotti (Eds.), Proceedings of the Symposium on High Temperature Materials Chemistry, Electrochemical Society, 1983, p. 105.

[17] J.P. Doench, R.A. Huggins, in: Z.A. Munir, D. Cubicciotti (Eds.), Proceedings of the Symposium on High Temperature Materials Chemistry, Electrochemical Society, 1983, p. 115.

[18] A. Anani, R.A. Huggins, in: J.-P. Gabano, Z. Takehara, P. Bro (Eds.), Proceedings of the Symposium on Primary and Secondary Ambient Temperature Lithium Batteries, Electrochemical Society, 1988, p. 635.

[19] A. Anani, R.A. Huggins, J. Power Sources 38 (1992) 351.

[20] R.A. Huggins, in: P. Vashishta, J.N. Mundy, G.K. Shenoy (Eds.), Fast Ion Transport in Solids, North-Holland, 1979, p. 53.

[21] C. J. Wen, Ph.D. Dissertation, Stanford University, (1980).

[22] I.D. Raistrick, R.A. Huggins, Mater. Res. Bull. 18 (1983) 337.

[23] I.D. Raistrick, A.J. Mark, R.A. Huggins, Solid State Ionics 5 (1981) 351.

[24] W. Weppner, R.A. Huggins, J. Electrochem. Soc. 124 (1977) 1569.

[25] W. Weppner, R.A. Huggins, in: R.A. Huggins (Ed.), Annual Review of Materials Science, Annual Reviews, Inc., 1978. p. 269.

[26] C.J. Wen, et al., Int. Met. Rev. 5 (1981) 253.

[27] C.J. Wen, et al., J. Electrochem. Soc. 126 (1979) 2258.

[28] C.J. Wen, et al., Met. Trans. B 11B (1980) 131.

[29] C.J. Wen, R.A. Huggins, J. Solid State Chem. 37 (1981) 271.

[30] C.J. Wen, R.A. Huggins, J. Electrochem. Soc. 128 (1981) 1181.

[31] C.J. Wen, R.A. Huggins, J. Solid State Chem. 35 (1980) 376.

[32] J.P. Doench, R.A. Huggins, J. Electrochem. Soc. 129 (1982) 341.

[33] J. Wang, I.D. Raistrick, R.A. Huggins, J. Electrochem. Soc. 133 (1986) 457.

[34] J. Wang, P. King, R.A. Huggins, Solid State Ionics 29 (1986) 185.

[35] A. Anani, S. Crouch-Baker, R.A. Huggins, in: A.N. Dey (Ed.), Proceedings of the Symposium on Lithium Batteries, Electrochemical Society, 1987, p. 365

[36] B.A. Boukamp, G.C. Lesh, R.A. Huggins, J. Electrochem. Soc. 128 (1981) 725.

[37] B.A. Boukamp, G.C. Lesh, R.A. Huggins, in: H.V. Venkatasetty (Ed.), Proceedings of the Symposium on Lithium Batteries, Electrochemical Society, 1981, p. 467.

[38] R. A. Huggins, B. A. Boukamp, U.S. Patent 4,436,796 (1984).

[39] A. Anani, S. Crouch-Baker, R.A. Huggins, in: A.N. Dey (Ed.), Proceedings of the Symposium on Lithium Batteries, Electrochemical Society, 1987, p. 382.

[40] A. Anani, S. Crouch-Baker, R.A. Huggins, J. Electrochem. Soc. 135 (1988) 2103.

[41] C.J. Wen, R.A. Huggins, Mater. Res. Bull. 15 (1980) 1225.

[42] M.L. Saboungi, et al., J. Electrochem. Soc. 126 (1979) 322.

[43] C.J. Wen, R.A. Huggins, J. Electrochem. Soc. 128 (1981) 1636.